Collapsed tetragonal phase as a strongly covalent and fully nonmagnetic state: persistent magnetism with interlayer As–As bond formation in Rh-doped Ca0.8Sr0.2Fe2As2

K. Zhao, J. K. Glasbrenner, H. Gretarsson, Dominik Schmitz, J. Bednarcik, M. Etter, J. P. Sun, Rudra S. Manna, A. Al-Zein, S. Lafuerza, Wolfgang Scherer, J. G. Cheng, Philipp Gegenwart

Angaben zur Veröffentlichung / Publication details:

Zhao, K., J. K. Glasbrenner, H. Gretarsson, Dominik Schmitz, J. Bednarcik, M. Etter, J. P. Sun, et al. 2018. "Collapsed tetragonal phase as a strongly covalent and fully nonmagnetic state: persistent magnetism with interlayer As–As bond formation in Rh-doped Ca0.8Sr0.2Fe2As2." *Physical Review B* 97 (2): 020510(R). https://doi.org/10.1103/physrevb.97.020510.

Rapid Communications

Collapsed tetragonal phase as a strongly covalent and fully nonmagnetic state: Persistent magnetism with interlayer As–As bond formation in Rh-doped $Ca_{0.8}Sr_{0.2}Fe_2As_2$

K. Zhao,[1] J. K. Glasbrenner,[2,3] H. Gretarsson,[4] D. Schmitz,[5] J. Bednarcik,[6] M. Etter,[6] J. P. Sun,[7] R. S. Manna,[1] A. Al-Zein,[8] S. Lafuerza,[8] W. Scherer,[5] J. G. Cheng,[7] and P. Gegenwart[1]

[1]*Experimentalphysik VI, Center for Electronic Correlations and Magnetism, University of Augsburg, 86159 Augsburg, Germany*
[2]*Department of Computational and Data Sciences, Computational Materials Science Center, George Mason University, 4400 University Drive, Fairfax, Virginia 22030, USA*
[3]*National Research Council/Code 6393, Naval Research Laboratory, Washington DC 20375, USA*
[4]*Max-Planck-Institut für Festkörperforschung, Heisenbergstraße 1, D-70569 Stuttgart, Germany*
[5]*CPM, Institute of Physics, University of Augsburg, 86135 Augsburg, Germany*
[6]*Deutsches Elektronen-Synchrotron (DESY), 22607 Hamburg, Germany*
[7]*Beijing National Laboratory for Condensed Matter Physics, Institute of Physics, Chinese Academy of Sciences, Beijing 100190, China*
[8]*European Synchrotron Radiation Facility, Boîte Postale 220, F-38043 Grenoble Cedex, France*

(Received 1 March 2017; revised manuscript received 23 August 2017; published 31 January 2018)

A well-known feature of the $CaFe_2As_2$-based superconductors is the pressure-induced collapsed tetragonal phase that is commonly ascribed to the formation of an interlayer As–As bond. Using detailed x-ray scattering and spectroscopy, we find that Rh-doped $Ca_{0.8}Sr_{0.2}Fe_2As_2$ does not undergo a first-order phase transition and that local Fe moments persist despite the formation of interlayer As–As bonds. Our density functional theory calculations reveal that the Fe–As bond geometry is critical for stabilizing magnetism and the pressure-induced drop in the c lattice parameter observed in pure $CaFe_2As_2$ is mostly due to a constriction within the FeAs planes. The collapsed tetragonal phase emerges when covalent bonding of strongly hybridized Fe $3d$ and As $4p$ states completely wins out over their exchange splitting. Thus the collapsed tetragonal phase is properly understood as a strong covalent phase that is fully nonmagnetic with the As–As bond forming as a by-product.

DOI: 10.1103/PhysRevB.97.020510

The pressure-induced collapsed tetragonal (CT) phase transition [1–3] of the iron-based superconductor $CaFe_2As_2$ [4,5] is a structural transition characterized by a discontinuous change in the material's lattice parameters and volume. The transition is unique among the $ThCr_2Si_2$ (122) structural family of iron-based superconductors [6–14], occurring at a hydrostatic pressure of 0.35 GPa [1] that is an order of magnitude lower than the continuous (second-order) transitions observed in the other members of the AFe_2As_2 (A = Ba,Sr,Eu) family [15,16]. The CT phase itself is nonmagnetic (NM), lacks magnetic fluctuations [2,17], exhibits Fermi-liquid behavior [18,19], and is not superconducting [20], which supports a spin-fluctuation model of superconductivity. There is a diversity of opinion on how to describe the Fe moment for the CT phase transition with most models belonging to one of three categories: (1) the magnetism is itinerant, and the Fe moment is quenched when a Fermi-surface nesting vector disappears due to pressure [21], (2) the magnetism is local, and the Fe moment is quenched when pressure-induced gains in the Gibb's free energy win out over the Hund's coupling [22], and (3) each Fe^{2+} site has six $3d$ electrons arranged in one of three distinct spin states, $S = 0$ (nonmagnetic), $S = 1$ (low spin), and $S = 2$ (high spin), and applying pressure transitions a majority of the Fe sites from $S = 2$ to $S = 0$ or $S = 1$, suppressing magnetism [23]. Regardless of the way one models the Fe magnetic moment, the driving mechanism of the CT phase is generally attributed to a well-known feature of the CT phase, the strong interlayer As–As covalent bond [24]. Stronger interlayer As–As bonds will promote shorter interlayer As–As bond lengths as Hoffman and Zheng showed in their bond analysis of the $ThCr_2Si_2$ structural compounds [25], and thus the CT phase transition occurs when the As–As bond length decreases below a critical value of 3 Å [26] at which point the As–As bonding energy wins out over the magnetic energy and induces a first-order structural transition that quenches the Fe moments.

These models face challenges when applied to $CaFe_2As_2$-based chemical substitution experiments [26,27]. Substituting 33% of Ca sites with Sr and applying pressure leads to a paramagnetic CT phase (defined here as a structure with an As–As bond length shorter than 3 Å) instead of a nonmagnetic one with a phase transition that is still unclear whether it is a first or second type [26,27]. A pure itinerant model cannot explain this paramagnetic CT phase, whereas the challenge for localized models is to provide an explanation for why identical cell volumes result in a paramagnetic phase for the Sr-doped case and a nonmagnetic phase for the undoped case. A localized model may be able to quantify the trend by fitting to electronic structure calculations, but this limits its explanatory power as this effectively includes itinerant features, whereas a mixed valence model as acknowledged in Ref. [23] cannot explain the first-order collapse to a nonmagnetic state and thus is unable to identify a mechanism for what Sr doping changes in the material.

A remarkable success of density functional theory (DFT) is that it can distinguish between the uncollapsed and the collapsed phases in the 122 family as structural relaxation calculations using a magnetic structure with $\mathbf{q} = (\pi,0)$ or $(0,\pi)$ [known as the single stripe (SS) pattern] reproduces the lattice parameters of the uncollapsed tetragonal phase, whereas relaxing in the nonmagnetic state reproduces the CT phase [24,28–32]. In terms of chemical bonding, both DFT [31] and DFT-based dynamical mean-field theory (DFT + DMFT) [33,34] calculations find that there is a substantial amount of hybridization between the Fe $3d$ and the As $4p$ states, which becomes *stronger* in the CT phase despite the formation of the As–As bond. In fact, the substantial Fe–As hybridization is a general feature of the pnictides [35]. In the magnetic uncollapsed phase, the Fe–As bonding and antibonding hybrid bands themselves are exchange split, leading to a competition between the covalent bonding and the magnetic energy reflected in the equilibrium distance between neighboring Fe and As planes. Increasing the exchange splitting weakens the covalent bond as electrons start to occupy the majority antibonding band, whereas reducing the exchange splitting empties the majority antibonding band and strengthens the covalent bond [35]. Indeed, the proximity of such antibonding states to the Fermi level was reported in the analysis of Hoffman and Zheng (here the bond is Mn–P) [25]. Furthermore, other key quantities in DFT + DMFT calculations, such as the d_{xy} orbital's imaginary part of the self-energy, are quite sensitive to the Fe–As bond geometry but not to the As–As bond length [34]. This mounting evidence seems to suggest that the CT phase transition has less to do with the As–As bond and more to do with the Fe–As bond geometry.

In this Rapid Communication, we report on the changes in the structural and magnetic properties of Sr- and Rh-doped $CaFe_2As_2$ using electrical resistivity, thermal expansion, x-ray diffraction, and x-ray emission spectroscopy (XES) measurements. Substituting Fe with Rh [19] provides chemical pressure, avoiding the challenges inherent in performing spectroscopic measurements under high pressures. We obtain the surprising result that Rh-doped $Ca_{0.8}Sr_{0.2}Fe_2As_2$ does not undergo a first-order phase transition and that the local Fe moments persist despite the formation of interlayer As–As bonds. Using DFT calculations, we demonstrate that subtle variations in the Fe–As bond geometry determines whether Fe is magnetic or not and that a first-order CT phase transition corresponds to the intralayer constriction of neighboring As–Fe–As planes due to quenching of magnetism. These results show a complexity that cannot be explained in models that require a sharp distinction between low-spin and high-spin states or that start from a fully localized or itinerant description. Instead, the same set of electrons both provide the local moments and form the Fe–As and As–As bonds, so we interpret our results using the framework of a competition between covalent bonds and exchange splitting [35]. In this picture, forming a covalent As–As bond does not require the quenching of magnetism, and the transition to the CT phase is allowed to be continuous, depending on the details of how the Fe–As bond geometry evolves with pressure. Furthermore, the CT phase is properly identified not by a sub-3-Å As–As bond length [26] but instead as a fully nonmagnetic phase with strong Fe–As and As–As covalent bonds. This framework provides a common mechanism for the nonmagnetic CT phase in $CaFe_2As_2$ and the other 122 materials [15,16].

TABLE I. Crystallographic data of $Ca_{0.8}Sr_{0.2}(Fe_{1-x}Rh_x)_2As_2$ ($x = 0.25$ and 0.48) and $Ca(Fe_{1-x}Rh_x)_2As_2$ ($x = 0.28$).

300 K	$Ca_{0.8}Sr_{0.2}(Fe_{1-x}Rh_x)_2As_2$ ($x = 0.25$ and 0.48)	$Ca(Fe_{1-x}Rh_x)_2As_2$ ($x = 0.28$)
	Lattice parameter (Å)	
a	3.9891(6)/4.06610(10)	4.0270(3)
c	11.2556(17)/10.6100(2)	10.6450(9)
	Atomic sites	
Ca(Sr)	$2a$ (0,0,0)	$2a$ (0,0,0)
Fe(Rh)	$4d$ (0,0.25,0.5)	$4d$ (0,0.25,0.5)
As	$4e$ [0,0,0.36579(5)/0.36806(5)]	$4e$ [0,0,0.36763(6)]
	Average bond lengths (Å)	
Fe–As	2.3826(4)/2.3880(3)	2.3711(4)
Fe–Fe	2.8207(4)/2.8752(1)	2.8475(2)
As–As	3.0213(12)/2.7998(12)	2.8181(13)
	Average bond angles (deg)	
As–Fe–As (θ)	113.68(2)/116.72(1)	116.25(3)
As–Fe–As (β)	107.410(12)/105.971(10)	106.194(12)

Figure 1(b) displays the phase diagram for $Ca_{0.8}Sr_{0.2}(Fe_{1-x}Rh_x)_2As_2$ ($0 < x < 0.48$), based on x-ray diffraction and spectroscopy, electrical resistivity, and thermal expansion, see the Supplemental Material [36] and Refs. [37,38] for more details. Upon Rh doping, bulk superconductivity emerges after the complete suppression of the antiferromagnetic orthorhombic phase with a maximal transition temperature of 21 K. More Rh doping likely suppresses the antiferromagnetic fluctuations, and the superconducting phase vanishes around $x = 0.20$. The linear decrease in the c-axis parameter with x at 300 K (cf. stars and right y axis) indicates the absence of a first-order transition, in contrast to the sharp drop of the c axis for $Ca(Fe_{1-x}Rh_x)_2As_2$ [36] due to the CT phase transition at 300 K in the latter material [19]. Based on the electrical resistivity measurements on $Ca_{0.8}Sr_{0.2}Fe_2As_2$ under hydrostatic pressure, a similar phase diagram compared to the Rh-doped case can be constructed [36,39], again without a first-order phase transition.

To investigate the structural details and atomic coordinates, single-crystal x-ray diffraction was conducted for $Ca_{0.8}Sr_{0.2}(Fe_{1-x}Rh_x)_2As_2$ ($x = 0.25$ and 0.48) [CaSr–Rh0.25 and CaSr–Rh0.48] and $Ca(Fe_{1-x}Rh_x)_2As_2$ ($x = 0.28$) [Ca–Rh0.28], yielding the results listed in Table I [36,40–43]. The geometry parameters of the $FeAs_4$ tetrahedra including the Fe–As bond length and the As–Fe–As angle are derived together with the interlayer As–As distance. For CaSr–Rh0.48, this As–As distance is 2.8 Å, similar to the value of Ca–Rh0.28. Note that both distances are less than the critical value of 3 Å [26]. Independent pair distribution function (PDF) measurements show the same formation of short interlayer As–As bonds in Ca–Rh0.28 and CaSr–Rh0.48 at 300 K, see the Supplemental Material [36] and Refs. [44–47]. Additionally the PDF measurements confirm that the Fe–As bond is enhanced for CaSr–Rh0.48 by about 0.01 Å compared to Ca–Rh0.28.

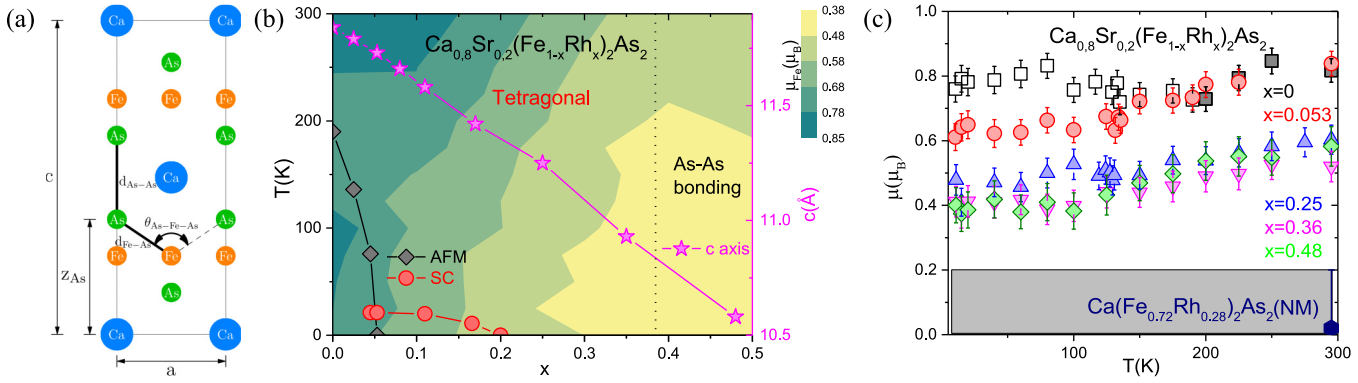

FIG. 1. (a) Side view of the crystal structure of $CaFe_2As_2$ with labels for the structural parameters. (b) Temperature composition x phase diagram for $Ca_{0.8}Sr_{0.2}(Fe_{1-x}Rh_x)_2As_2$ with the size of Fe moments as determined from x-ray emission spectroscopy. The diamonds and filled circles indicate the antiferromagnetic and superconducting transitions, respectively, determined from electrical resistivity and thermal expansion. The pink stars indicate the size of the c-lattice parameter at room temperature (right y axis) which decreases linearly to values characteristic for the interlayer As–As bonding beyond $x = 0.38$, cf. cyan dotted vertical line. (c) Temperature dependence of the Fe local moment μ (μ_B) for $Ca_{0.8}Sr_{0.2}(Fe_{1-x}Rh_x)_2As_2$ ($x = 0$, 0.053, 0.25, 0.36, and 0.48) derived from respective XES spectra as described in text. The open square represents the local moment in an antiferromagnetic order state. The local moment for $Ca(Fe_{1-x}Rh_x)_2As_2$ ($x = 0.28$) is also shown for comparison.

To investigate the link between the structure of $Ca_{0.8}Sr_{0.2}(Fe_{1-x}Rh_x)_2As_2$ and its fluctuating Fe moment [23,48–50], we measured the temperature and doping dependence of the Fe $K\beta$ emission line, see the Supplemental Material [36] and Refs. [51–56] for technical details. By application of the integrated absolute difference (IAD) analysis on the shape of the emission line, information on the size of the Fe magnetic moment can be obtained [36]. In Fig. 1(c), we plot the temperature dependence of the local moment for $Ca_{0.8}Sr_{0.2}(Fe_{1-x}Rh_x)_2As_2$ ($x = 0$, 0.053, 0.25, 0.36, and 0.48), extracted from the emission line as described above. The detection limit (zero signal) of the IAD technique is shown by the shaded area [23]. At room temperature the samples with lower Rh doping ($x = 0$ and $x = 0.053$) have a local moment around $0.8\mu_B$, which upon cooling gradually decreases to around $0.6\mu_B$. However, for $x = 0$, the moment starts to increase below the Néel temperature until the room-temperature value is reached again. The higher-doped samples for which interlayer As–As bonds are formed, show a finite but reduced moment of around $0.6\mu_B$ at room temperature. Upon cooling, this moment also gradually decreases from $\approx 0.6\mu_B$ at $T = 295$ K to $0.4\mu_B$ at 10 K. This observation is in stark contrast to our results on Ca–Rh0.28, which shows a nonmagnetic state at 300 K.

To understand why the magnetism persists for CaSr–Rh0.48 despite the As–As bond length being close in value to the pressure-induced CT phase of undoped $CaFe_2As_2$ ($d_{As-As} = 2.7952$ Å) [1], we performed a series of DFT calculations using the pseudopotential software package VASP with projector augmented-wave potentials [57,58] and the generalized gradient approximation exchange-correlation functional [59], see the Supplemental Material [36] and Ref. [60] for details. We found that subtle changes in the lattice parameters due to chemical pressure affect the magnetic stability. Fixing the lattice parameters to the Ca–Rh0.28 values reported in Table I weakens the magnetic stability, and magnetism is fully suppressed with a Rh-doping level of 25% or higher. In contrast, using the CaSr–Rh0.48 values stabilizes magnetism with the antiferromagnetic SS phase remaining stable up to 25% Rh doping, and the Fe local moment was still present at 50% Rh doping, see the Supplemental Material [36].

Next, we assessed the role of the Fe–As bond in stabilizing magnetism using a second set of DFT calculations that interpolated between the CaSr–Rh0.48 and the Ca–Rh0.28 lattice parameters in a two-stage process (the As–As bond length was fixed to its Ca–Rh0.28 value), see Fig. 2. We found that in the absence of electron doping that a 0.72% reduction in the Fe–As bond length increases the energy of the magnetic phase relative to the nonmagnetic phase by nearly a factor of 2. Furthermore, with 25% Rh doping the system transitions to a nonmagnetic phase at a Fe–As bond length of 2.37522 Å as the SS phase becomes metastable. The As–Fe–As bond angle is relatively unchanged in the interpolation, however in a separate calculation we found that increasing the angle by 1.3° lowered the energy by ∼10 meV. This confirms that even in this "collapsed" environment that small changes in the Fe–As bond geometry affect the stability of the magnetic phase.

These results show a sharp division between two phases (one magnetic and the other fully nonmagnetic) that depends on the geometry of the Fe–As bond even when the As–As bond length is <3 Å, which presents a serious challenge to the theory that forming an As–As bond *drives* the CT phase transition. One possible objection to this would be that we have only shown this to hold for characteristics that might be specific to doped $CaFe_2As_2$. To address this, we performed structural relaxation calculations of undoped $CaFe_2As_2$ for a series of fixed volumes. The resulting bond lengths (Fe–As and As–As) and bond angle (As–Fe–As) as a function of cell volume are plotted in Fig. 2(c) with the CT phase transition occurring between the volumes $0.958V_0^{exp}$ and $0.968V_0^{exp}$ (V_0^{exp} is the experimental volume at ambient pressure [61]), which appears as a discontinuous 5.5% reduction in the c parameter. What has not been pointed out in previous discussions is that 83% of the c parameter's decrease is due to a change in the Fe–As

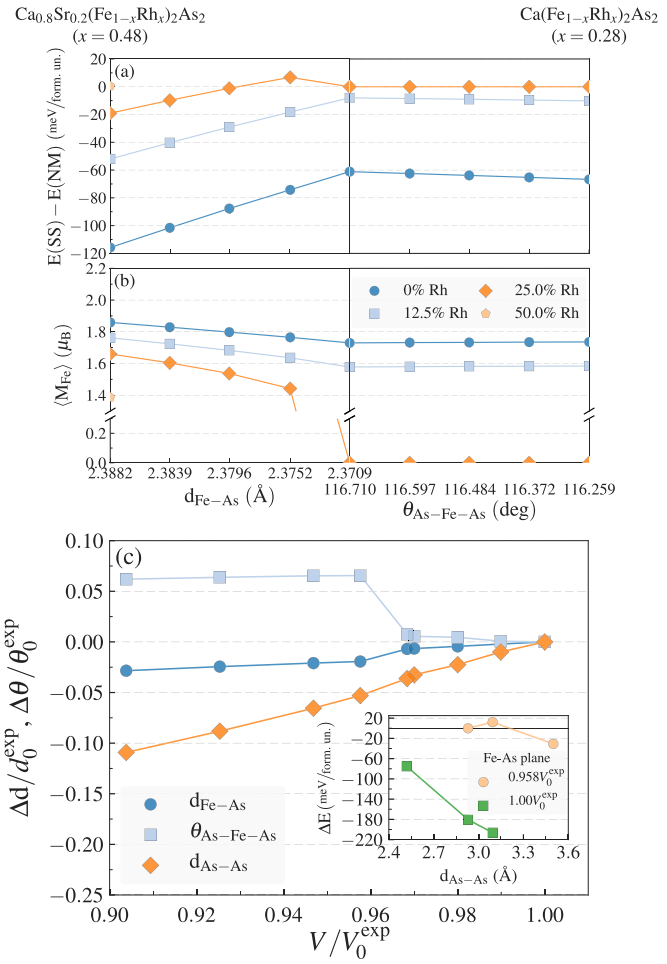

FIG. 2. Density functional theory calculations of the energy difference among the SS, the NM states [panel (a)], and the average Fe local moment [panel (b)] as you interpolate between the structural parameters for CaSr–Rh0.48 (far left) and Ca–Rh0.28 (far right), starting with $d_{\mathrm{Fe-As}}$ first and $\theta_{\mathrm{As-Fe-As}}$ second. In panel (c) the optimized structural parameters of pure $CaFe_2As_2$ are plotted as a function of the volume per formula unit. The reference point for the fractional volume and bond lengths/angle is the optimized structure for the experimental volume. The inset: The energy difference $\Delta E = E(\mathrm{SS}) - E(\mathrm{NM})$ at volumes constrained to 95.8% and 100% of the experimental volume when the FeAs plane geometry is fixed and $d_{\mathrm{As-As}}$ is varied.

bond geometry (mostly stemming from a 6% increase in the bond angle) with the remaining 17% due to a decrease in the As–As interlayer distance. Put another way, the collapse of the c parameter is the consequence of a *sudden constriction of the interlayer distance between neighboring Fe and As planes*, which occurs when magnetism is fully suppressed. This is not to say that the As–As bond plays no role; the inset of Fig. 2(c) shows that, if one fixes the FeAs plane geometry of the collapsed $0.958V_0^{\mathrm{exp}}$ structure and artificially increases the interlayer As–As distance, then this will restore the magnetic phase [62]. So, what we have found is that the As–As bond works against magnetism and lowers the critical pressure compared to an isolated FeAs plane, but its formation is not necessary or sufficient to *drive* the transition to the CT state.

So what is the nature of the CT phase? We have established that the phase transition occurs when magnetism is fully suppressed, causing the FeAs planes to constrict, and that there is a direct connection between the stability of magnetism and the Fe–As bond geometry. As discussed earlier, the mechanism determining the equilibrium Fe–As bond geometry was identified in Ref. [35] as a competition between covalent bonding (disfavoring magnetism) and exchange splitting (favoring magnetism) of the hybridized Fe $3d$ and As $4p$ states. Hence, the CT phase should be viewed as a fully nonmagnetic *strong covalent phase* that manifests due to covalency winning out in the Fe–As bonds [33] with increasing pressure.

Understanding that the CT phase is the product of a strong covalent Fe–As bond that fully suppresses magnetism offers insight on other results in the literature. First, a 122 pnictide is not in the CT phase if magnetism coexists with an As–As interlayer distance that is below 3 Å (an example is applying pressure to 33% Sr-doped $CaFe_2As_2$ [27]). Second, there does not seem to be a requirement that the CT phase transition is first order. In the case of Sr-doped $CaFe_2As_2$, according to our hydrostatic pressure measurements (see the Supplemental Material [36]) and Ref. [63], the phase transition remains first order only when Sr doping remains low (<17.7%), whereas at higher dopings there is a sudden, yet continuous, increase in the As–Fe–As bond angle with increasing pressure as magnetism becomes suppressed. This kind of second-order phase-transition behavior is also seen in $BaFe_2As_2$ [16], and so we conclude that: (1) the CT phase is a general feature of the 122 family of pnictides and (2) the critical pressure for the 300-K measurements in Ref. [16] is determined by where the As–Fe–As bond angle plateaus, which is at 36 GPa instead of the quoted estimate of 27 GPa. Finally, it is worth noting that in rare-earth-doped $CaFe_2As_2$ a superconducting state above 45 K emerges at the same time as a CT phase transition [64–66]. Our results show that first-order CT phase transitions are the result of a sudden quench of magnetism, which suggests that the CT phase in combination with a higher superconducting temperature are likely correlated in these materials. Further investigations in this direction are needed.

To summarize, our Fe $K\beta$ x-ray emission spectroscopy and DFT calculations establish the coexistence of local Fe moments with an interlayer As–As covalent bond with a length smaller than 3 Å in Rh-doped $Ca_{0.8}Sr_{0.2}Fe_2As_2$. We find that the collapsed tetragonal phase is properly identified by a sudden constriction within the FeAs planes that occurs when magnetism is suppressed, which is due to covalent bonding between the hybridized Fe $3d$ and the As $4p$ states winning out over exchange splitting. Therefore the collapsed tetragonal phase is not driven by forming an As–As bond and is instead a nonmagnetic and strongly covalent phase that should be distinguished from other magnetic or paramagnetic phases, even if under certain conditions they have relatively similar lattice parameters.

The authors would like to thank I. I. Mazin for helpful discussions and critical comments. K.Z. thanks Q. H. Zhang for the EDX measurement and the Alexander von Humboldt Foundation for support. Financial support by the German Science Foundation through the priority program SPP1458

is acknowledged. J.K.G. acknowledges the support of the National Research Council Program at Naval Research Laboratory. Parts of this research were carried out at the light source PETRA III (beamline P02.1) at DESY, a member of the Helmholtz Association. J.G.C. was supported by the National Science Foundation of China (Grant No. 11574377), the National Basic Research Program of China (Grant No. 2014CB921500), the Strategic Priority Research Program and Key Research Program of Frontier Sciences of the Chinese Academy of Sciences (Grants No. XDB07020100 and No. QYZDBSSW-SLH013).

K.Z. and J.K.G. contributed equally to this work.

[1] A. Kreyssig, M. A. Green, Y. Lee, G. D. Samolyuk, P. Zajdel, J. W. Lynn, S. L. Bud'ko, M. S. Torikachvili, N. Ni, S. Nandi, J. B. Leão, S. J. Poulton, D. N. Argyriou, B. N. Harmon, R. J. McQueeney, P. C. Canfield, and A. I. Goldman, Phys. Rev. B **78**, 184517 (2008).

[2] A. I. Goldman, A. Kreyssig, K. Prokeš, D. K. Pratt, D. N. Argyriou, J. W. Lynn, S. Nandi, S. A. J. Kimber, Y. Chen, Y. B. Lee, G. Samolyuk, J. B. Leão, S. J. Poulton, S. L. Bud'ko, N. Ni, P. C. Canfield, B. N. Harmon, and R. J. McQueeney, Phys. Rev. B **79**, 024513 (2009).

[3] P. C. Canfield, S. L. Bud'ko, N. Ni, A. Kreyssig, A. I. Goldman, R. J. McQueeney, M. S. Torikachvili, D. N. Argyriou, G. Luke, and W. Yu, Phys. C **469**, 404 (2009).

[4] N. Ni, S. Nandi, A. Kreyssig, A. I. Goldman, E. D. Mun, S. L. Bud'ko, and P. C. Canfield, Phys. Rev. B **78**, 014523 (2008).

[5] F. Ronning, T. Klimczuk, E. D. Bauer, H. Volz, and J. D. Thompson, J. Phys.: Condens. Matter **20**, 322201 (2008).

[6] Y. Kamihara, T. Watanabe, M. Hirano, and H. Hosono, J. Am. Chem. Soc. **130**, 3296 (2008).

[7] X. H. Chen, T. Wu, G. Wu, R. H. Liu, H. Chen, and D. F. Fang, Nature (London) **453**, 761 (2008).

[8] G. F. Chen, Z. Li, D. Wu, G. Li, W. Z. Hu, J. Dong, P. Zheng, J. L. Luo, and N. L. Wang, Phys. Rev. Lett. **100**, 247002 (2008).

[9] M. Rotter, M. Tegel, and D. Johrendt, Phys. Rev. Lett. **101**, 107006 (2008).

[10] H. S. Jeevan, Z. Hossain, D. Kasinathan, H. Rosner, C. Geibel, and P. Gegenwart, Phys. Rev. B **78**, 092406 (2008).

[11] X. C. Wang, Q. Q. Liu, Y. X. Lv, W. B. Gao, L. X. Yang, R. C. Yu, F. Y. Li, and C. Q. Jin, Solid State Commun. **148**, 538 (2008).

[12] F.-C. Hsu, J.-Y. Luo, K.-W. Yeh, T.-K. Chen, T.-W. Huang, P. M. Wu, Y.-C. Lee, Y.-L. Huang, Y.-Y. Chu, D.-C. Yan, and M.-K. Wu, Proc. Natl. Acad. Sci. USA **105**, 14262 (2008).

[13] J. Paglione and R. L. Greene, Nat. Phys. **6**, 645 (2010).

[14] P. J. Hirschfeld, M. M. Korshunov, and I. I. Mazin, Rep. Prog. Phys. **74**, 124508 (2011).

[15] W. Uhoya, A. Stemshorn, G. Tsoi, Y. K. Vohra, A. S. Sefat, B. C. Sales, K. M. Hope, and S. T. Weir, Phys. Rev. B **82**, 144118 (2010).

[16] R. Mittal, S. K. Mishra, S. L. Chaplot, S. V. Ovsyannikov, E. Greenberg, D. M. Trots, L. Dubrovinsky, Y. Su, T. Brueckel, S. Matsuishi, H. Hosono, and G. Garbarino, Phys. Rev. B **83**, 054503 (2011).

[17] J. H. Soh, G. S. Tucker, D. K. Pratt, D. L. Abernathy, M. B. Stone, S. Ran, S. L. Bud'ko, P. C. Canfield, A. Kreyssig, R. J. McQueeney, and A. I. Goldman, Phys. Rev. Lett. **111**, 227002 (2013).

[18] S. Kasahara, T. Shibauchi, K. Hashimoto, Y. Nakai, H. Ikeda, T. Terashima, and Y. Matsuda, Phys. Rev. B **83**, 060505 (2011).

[19] M. Danura, K. Kudo, Y. Oshiro, S. Araki, T. C. Kobayashi, and M. Nohara, J. Phys. Soc. Jpn. **80**, 103701 (2011).

[20] W. Yu, A. A. Aczel, T. J. Williams, S. L. Bud'ko, N. Ni, P. C. Canfield, and G. M. Luke, Phys. Rev. B **79**, 020511 (2009).

[21] Y.-Z. Zhang, H. C. Kandpal, I. Opahle, H. O. Jeschke, and R. Valentí, Phys. Rev. B **80**, 094530 (2009).

[22] W. Ji, X.-W. Yan, and Z.-Y. Lu, Phys. Rev. B **83**, 132504 (2011).

[23] H. Gretarsson, S. R. Saha, T. Drye, J. Paglione, J. Kim, D. Casa, T. Gog, W. Wu, S. R. Julian, and Y.-J. Kim, Phys. Rev. Lett. **110**, 047003 (2013).

[24] T. Yildirim, Phys. Rev. Lett. **102**, 037003 (2009).

[25] R. Hoffmann and C. Zheng, J. Phys. Chem. **89**, 4175 (1985).

[26] J. R. Jeffries, N. P. Butch, K. Kirshenbaum, S. R. Saha, G. Samudrala, S. T. Weir, Y. K. Vohra, and J. Paglione, Phys. Rev. B **85**, 184501 (2012).

[27] J. R. Jeffries, N. P. Butch, M. J. Lipp, J. A. Bradley, K. Kirshenbaum, S. R. Saha, J. Paglione, C. Kenney-Benson, Y. Xiao, P. Chow, and W. J. Evans, Phys. Rev. B **90**, 144506 (2014).

[28] M. Tomić, R. Valentí, and H. O. Jeschke, Phys. Rev. B **85**, 094105 (2012).

[29] Y. Wang, Y. Ding, and J. Ni, Solid State Commun. **149**, 2125 (2009).

[30] N. Colonna, G. Profeta, A. Continenza, and S. Massidda, Phys. Rev. B **83**, 094529 (2011).

[31] M. Widom and K. Quader, Phys. Rev. B **88**, 045117 (2013).

[32] S. L. Bud'ko, X. Ma, M. Tomić, S. Ran, R. Valentí, and P. C. Canfield, Phys. Rev. B **93**, 024516 (2016).

[33] J. Diehl, S. Backes, D. Guterding, H. O. Jeschke, and R. Valentí, Phys. Rev. B **90**, 085110 (2014).

[34] A. van Roekeghem, P. Richard, X. Shi, S. Wu, L. Zeng, B. Saparov, Y. Ohtsubo, T. Qian, A. S. Sefat, S. Biermann, and H. Ding, Phys. Rev. B **93**, 245139 (2016).

[35] K. D. Belashchenko and V. P. Antropov, Phys. Rev. B **78**, 212505 (2008).

[36] See Supplemental Material at http://link.aps.org/supplemental/10.1103/PhysRevB.97.020510 for additional details about our x-ray diffraction, resistivity, and thermal expansion measurements, resistivity measurements of Sr-doped $CaFe_2As_2$ under hydrostatic pressure, Fe $K\beta$ x-ray emission spectra, measurements of the pairing distribution function, and density functional theory calculations.

[37] K. Zhao, C. Stingl, R. S. Manna, C. Q. Jin, and P. Gegenwart, Phys. Rev. B **92**, 235132 (2015).

[38] R. Küchler, T. Bauer, M. Brando, and F. Steglich, Rev. Sci. Instrum. **83**, 095102 (2012).

[39] J.-G. Cheng, K. Matsubayashi, S. Nagasaki, A. Hisada, T. Hirayama, M. Hedo, H. Kagi, and Y. Uwatoko, Rev. Sci. Instrum. **85**, 093907 (2014).

[40] Bruker AXS Inc., SAINT, version 8.34 A, Madison (WI), USA, 2013.

[41] G. M. Sheldrick, SADABS, version 2014/2, Göttingen, 2014.

[42] G. M. Sheldrick, Acta Crystallogr. Sect. A **64**, 112 (2008).

[43] G. M. Sheldrick, Acta Crystallogr. Sect. C **71**, 3 (2015).

[44] H. F. Poulsen, J. Neuefeind, H.-B. Neumann, J. R. Schneider, and M. D. Zeidler, J. Non-Cryst. Solids **188**, 63 (1995).
[45] T. Egami and S. J. L. Billinge, *Underneath the Bragg Peaks: Structural Analysis of Complex Materials*, 1st ed. (Pergamon, Oxford, UK, 2003), Vol. 16.
[46] A. P. Hammersley, S. O. Svensson, M. Hanfland, A. N. Fitch, and D. Hausermann, High Press. Res. **14**, 235 (1996).
[47] X. Qiu, J. W. Thompson, and S. J. L. Billinge, J. Appl. Crystallogr. **37**, 678 (2004).
[48] H. Gretarsson, A. Lupascu, J. Kim, D. Casa, T. Gog, W. Wu, S. R. Julian, Z. J. Xu, J. S. Wen, G. D. Gu, R. H. Yuan, Z. G. Chen, N.-L. Wang, S. Khim, K. H. Kim, M. Ishikado, I. Jarrige, S. Shamoto, J.-H. Chu, I. R. Fisher, and Y.-J. Kim, Phys. Rev. B **84**, 100509 (2011).
[49] L. Ortenzi, H. Gretarsson, S. Kasahara, Y. Matsuda, T. Shibauchi, K. D. Finkelstein, W. Wu, S. R. Julian, Y.-J. Kim, I. I. Mazin, and L. Boeri, Phys. Rev. Lett. **114**, 047001 (2015).
[50] S. Lafuerza, H. Gretarsson, F. Hardy, T. Wolf, C. Meingast, G. Giovannetti, M. Capone, A. S. Sefat, Y.-J. Kim, P. Glatzel, and L. de' Medici, Phys. Rev. B **96**, 045133 (2017).
[51] G. Vankó, T. Neisius, G. Molnár, F. Renz, S. Kárpáti, A. Shukla, and F. M. F. de Groot, J. Phys. Chem. B **110**, 11647 (2006).
[52] K. Tsutsumi, H. Nakamori, and K. Ichikawa, Phys. Rev. B **13**, 929 (1976).
[53] G. Peng, F. M. F. deGroot, K. Haemaelaeinen, J. A. Moore, X. Wang, M. M. Grush, J. B. Hastings, D. P. Siddons, and W. H. Armstrong, J. Am. Chem. Soc. **116**, 2914 (1994).
[54] W. Wu, A. McCollam, I. Swainson, P. M. C. Rourke, D. G. Rancourt, and S. R. Julian, Europhys. Lett. **85**, 17009 (2009).
[55] S. Ishida, T. Takiguchi, S. Fujii, and S. Asano, Physica B **217**, 87 (1996).
[56] G. Vankó, J.-P. Rueff, A. Mattila, Z. Németh, and A. Shukla, Phys. Rev. B **73**, 024424 (2006).
[57] G. Kresse and J. Hafner, Phys. Rev. B **47**, 558 (1993).
[58] G. Kresse and J. Furthmüller, Phys. Rev. B **54**, 11169 (1996).
[59] J. P. Perdew, K. Burke, and M. Ernzerhof, Phys. Rev. Lett. **77**, 3865 (1996).
[60] S. P. Ong, W. D. Richards, A. Jain, G. Hautier, M. Kocher, S. Cholia, D. Gunter, V. L. Chevrier, K. A. Persson, and G. Ceder, Comput. Mater. Sci. **68**, 314 (2013).
[61] A. I. Goldman, D. N. Argyriou, B. Ouladdiaf, T. Chatterji, A. Kreyssig, S. Nandi, N. Ni, S. L. Bud'ko, P. C. Canfield, and R. J. McQueeney, Phys. Rev. B **78**, 100506 (2008).
[62] This only holds near the CT phase transition. At lower volumes, such as $0.904\,V_0^{\mathrm{exp}}$, increasing the As–As interlayer distance does not restore magnetism.
[63] S. Knöner, E. Gati, S. Köhler, B. Wolf, U. Tutsch, S. Ran, M. S. Torikachvili, S. L. Bud'ko, P. C. Canfield, and M. Lang, Phys. Rev. B **94**, 144513 (2016).
[64] S. R. Saha, N. P. Butch, T. Drye, J. Magill, S. Ziemak, K. Kirshenbaum, P. Y. Zavalij, J. W. Lynn, and J. Paglione, Phys. Rev. B **85**, 024525 (2012).
[65] B. Lv, L. Deng, M. Gooch, F. Wei, Y. Sun, J. K. Meen, Y.-Y. Xue, B. Lorenz, and C.-W. Chu, Proc. Natl. Acad. Sci. USA **108**, 15705 (2011).
[66] K. Gofryk, M. Pan, C. Cantoni, B. Saparov, J. E. Mitchell, and A. S. Sefat, Phys. Rev. Lett. **112**, 047005 (2014).